



1 **Multiscale soil moisture estimates using static and roving** 2 **cosmic-ray soil moisture sensors**

3
4 David McJannet¹, Aaron Hawdon², Brett Baker², Luigi Renzullo³, Ross Searle¹

5
6 ¹CSIRO Land and Water, EcoSciences Precinct, Dutton Park, QLD, Australia

7 ²CSIRO Land and Water, ATSIP, James Cook University, QLD, Australia

8 ³CSIRO Land and Water, Canberra, ACT, Australia

9
10 *Correspondence to:* David McJannet (david.mcjannet@csiro.au)

11
12 **Abstract.** Soil moisture plays a critical role in land surface processes and as such there has been a recent
13 increase in the number and resolution of satellite soil moisture observations and development of land surface
14 process models with ever increasing resolution. Despite these developments, validation and calibration of these
15 products has been limited because of a lack of observations at corresponding scales. A recently developed
16 mobile soil moisture monitoring platform, known as the 'rover', offers opportunities to overcome this scale
17 issue. This paper describes a research project aimed at producing soil moisture estimates at a range of scales that
18 are commensurate with model and satellite retrievals. Our investigation involved static cosmic ray neutron
19 sensors and rover surveys across both broad (36 x 36 km at 9 km resolution) and intensive (10 x 10 km at 1 km
20 resolution) scales in a cropping district in the Mallee region of Victoria, Australia. We describe approaches for
21 converting rover survey neutron counts to soil moisture and discuss the factors controlling soil moisture
22 variability. Measurements revealed that temporal patterns in soil moisture were preserved through time and
23 regression modelling approaches were utilised to produce time series of property scale soil moisture which may
24 also have application in calibration and validation studies or local farm management. Intensive scale rover
25 surveys produced reliable soil moisture estimates at 1 km resolution while broad scale surveys produced soil
26 moisture estimates at 9 km resolution. We conclude that the multiscale soil moisture products produced in this
27 study are well suited to future analysis of satellite soil moisture retrievals and finer scale soil moisture models.

28 **1 Introduction**

29 Soil moisture has a strong influence of land-atmosphere interactions, hydrological processes, ecosystem
30 functioning and agricultural productivity. The importance of this variable has led to an increase in the number
31 and resolution of satellite soil moisture observations and the ongoing development of finer resolution land
32 surface process models (Ochsner et al., 2013). Despite these developments, our ability to validate and/or
33 calibrate these products is limited because of a lack of observations at matching scales. Satellite observations
34 typically have resolutions in the order of 3 to 50 km, while broad-area modelling of soil moisture variability
35 typically occurs at resolutions >1 km. The scale of these products are orders of magnitude larger than those of
36 traditional in situ sensors which creates an issue because of the well documented small scale variability in soil
37 moisture (Vereecken et al., 2014; Western and Blöschl, 1999). Some researchers have overcome this issue by



38 establishing soil moisture monitoring networks (Bogena et al., 2010; Smith et al., 2012), but the extent of sensor
39 networks is still relatively small (<1 km²).

40

41 More recently cosmic-ray neutron sensors (CRNS) have been deployed to provide soil moisture estimates at a
42 scale hectometres (circular footprint, 260-600 m diameter) (Desilets and Zreda, 2013; Köhli et al., 2015). CRNS
43 sensors measure naturally generated fast neutrons (energy 10–1000 eV) that are produced by cosmic rays
44 passing through the Earth's atmosphere. The neutron intensity above the soil surface is inversely correlated with
45 soil moisture as it responds to the hydrogen contained in the soil and plant water and to a lesser degree to plant
46 and soil carbon compounds (Desilets et al., 2010). The better scale match between the CRNS technique and
47 satellite observations has led to a number of recent studies which compare CRNS observations to satellite
48 observations and modelled soil moisture (e.g. Montzka et al., 2017; Vinodkumar et al., 2017; Holgate et al.,
49 2016; Renzullo et al., 2014; Kędzior and Zawadzki, 2016). Development of networks of CRNS across a number
50 of countries (e.g. USA (Zreda et al., 2012), UK (Evans et al., 2016), Germany (Baatz et al., 2014), and Australia
51 (Hawdon et al., 2014)) is providing useful time series of soil moisture information which will be valuable for
52 years to come.

53

54 While the CRNS provides a better match to the scale of satellite retrievals and model estimates there is still a
55 scale mismatch that prevents direct full-scale validation of these products. To address this, a mobile CRNS,
56 called the cosmic-ray rover has been developed (Desilets et al., 2010). The rover uses the same technology as
57 the CRNS but its design allows for mobile mapping of soil moisture across the landscape. This mobile mapping
58 capability allows for soil moisture surveys to be undertaken over areas commensurate with satellite pixels or
59 model domains thereby filling the gap in soil moisture observations (Chrisman and Zreda, 2013). The earliest
60 use of the cosmic-ray rover was for repeated surveys across an area of 25 x 40 km in the Tucson Basin in order
61 to produce a catchment scale water balance (Chrisman and Zreda, 2013). Dong et al. (2014) used a rover to map
62 soil moisture on multiple occasions over a 16 x 10 km and a 34 x 14 km region in Oklahoma with the aim of
63 evaluating satellite soil moisture estimates. More recently Franz et al. (2015) combined rover surveys over a 12
64 x 12 km area in Nebraska with CRNS measurements to develop a technique for multiscale real-time soil
65 moisture monitoring.

66

67 This paper describes part of a research project aimed at producing soil moisture estimates at a range of scales for
68 eventual comparison to satellite and modelled soil moisture estimates. The focus of this paper is on establishing
69 techniques for producing spatial representations of soil moisture using CRNS sensors and a cosmic-ray rover.

70 We will present a nested set of broad scale and intensive scale rover survey results which were collected across
71 a 36 x 36 km area in a cropping district in Mallee region of Victoria, Australia and we will describe techniques
72 used to convert rover measurements into soil moisture estimates using CRNS sensors and spatial soil property
73 information. Using statistical relationships between property scale soil moisture from rover surveys and CRNS
74 sensors we will present a simple approach for producing real-time property-scale soil moisture estimates in the
75 local area. We also use our observations at different scales to test the reliability of our experimental design.

76 **2 Methods**77 **2.1 Site description**

78 The study area is located in the Shire of Buloke in the Mallee region of Victoria, Australia (Figure 1). The
79 measurement campaign took place across a 36 x 36 km region centred on -35.684°S, 142.858°E, which lies
80 between the towns of Birchip to the south and Sea Lake to the north. The Mallee is a rain fed agricultural region
81 with wheat and barley being widely grown. Much of the native vegetation has been removed since European
82 settlement. In the region of interest the landscape is flat with an elevation ranging between 50 to 120 m ASL.
83 The climate of the area is classified as semi-arid with an average annual rainfall of 368 mm, an average
84 minimum temperature in July of 3.6°C and an average maximum temperature in January of 30.7°C (Anwar et
85 al., 2007).

86 **2.2 Static cosmic-ray soil moisture sensors**

87 Cosmic-ray soil moisture sensors were installed at two locations in the designated field survey area (Figure 1).
88 These two locations are named Bishes (northern probe) and Bennetts (southern probe). Each of these sensors
89 included a single polyethylene shielded cosmic-ray probe (CRP-1000B, Hydroinnova, Albuquerque, USA),
90 which monitors neutron intensity in the epithermal to fast neutron energy range. Each system also measured
91 barometric pressure, temperature and relative humidity, which are required for measurement correction
92 procedures. The system was programmed to record data at hourly intervals and was sent via satellite telemetry
93 (Iridium SBD services) in near-real-time to a database on a remote server (cosmoz.csiro.au).

94

95 In order to isolate the effect of soil moisture on neutron count measurements it is first necessary to remove
96 variation due to other environmental factors. The largest correction that is required is an adjustment for changes
97 in atmospheric pressure, but there are also corrections required for changes in atmospheric water vapor and
98 changes in the intensity of the incoming neutron flux. The standard correction procedures implemented across
99 the CosmOz network have been described in detail by Hawdon et al. (2014) therefore only a brief summary will
100 be provided here.

101

102 Cosmic-ray neutron intensity is particularly sensitive to elevation or the mass of air above the sensor, which is
103 defined as an exponential relationship with barometric pressure (Zreda et al., 2008);

$$104 \quad f_p = \exp[\beta(P - P_{ref})] \quad \text{Eq. 1}$$

105 where P is atmospheric pressure (mb) and P_{ref} is the reference atmospheric pressure (mb); which is calculated
106 using standard formulas based on site elevation (NASA, 1976). The atmospheric attenuation coefficient (β ,
107 $\text{cm}^2 \text{g}^{-1}$ or mb^{-1}) for neutron-generating cosmic rays has been calculated for each of our sites using the method
108 described by Desilets et al. (2006).

109

110 Water vapor in the atmosphere has the same neutron moderating capacity as water in the soil and as such will
111 influence the total neutron count (Zreda et al., 2012). A correction factor for atmospheric water vapor effects
112 was developed by Rosolem et al. (2013) and it utilises near surface absolute humidity (ρ_{v0} , g m^{-3}), which is



113 derived from measurements of temperature, atmospheric pressure and humidity. The correction factor for
114 atmospheric water vapor (f_{ww}) is derived from;

$$115 \quad f_{ww} = 1 + 0.0054(\rho_{v0} - \rho_{v0}^{ref}) \quad \text{Eq. 2}$$

116 where ρ_{v0}^{ref} is the reference absolute humidity, which we set to 0 g m^{-3} (i.e. dry air).

117 To account for variations in incoming neutron flux an intensity correction factor is calculated by normalising the
118 source intensity to a fixed point in time (Zreda et al., 2012). The correction factor for incoming neutron intensity
119 (f_i) is expressed as;

$$120 \quad f_i = \frac{I_m}{I_{ref}} \quad \text{Eq. 3}$$

121 where I_m is the selected neutron monitor counting rate at any particular point in time and I_{ref} is a reference
122 counting rate for the same neutron monitor from an arbitrary fixed point in time which is 1 May 2011. Neutron
123 monitor data is sourced from the Neutron Monitor Database (NMDB; www.nmdb.eu). Both of these sites utilise
124 data from the Lomnický štít Observatory in Slovakia.

125

126 The counting rate is also scaled to sea level and high latitude to enable comparison between sensors. Scaling
127 factors for converting counting rate to sea level (f_s) and high latitude (f_l) are described by Desilets and Zreda
128 (2003) and Desilets et al. (2006).

129

130 Final corrected counts (N) are calculated using the following equation;

$$131 \quad N = N_{raw} \left(\frac{f_p f_{ww}}{f_i} \right) \left(\frac{f_s}{f_l} \right) \quad \text{Eq. 4}$$

132 Where N_{raw} is the uncorrected neutron count from the CRP. Corrected neutron counts were converted to
133 volumetric soil moisture content (θ) using the calibration function generated by Desilets et al. (2010) and
134 modified by Bogen et al. (2013):

$$135 \quad \theta = \left(\frac{0.0808}{\left(\frac{N}{N_0} \right) - 0.372} - 0.115 - W_{lat} - W_{SOC} \right) \rho_{bd} \quad \text{Eq. 5}$$

136 where N_0 is the neutron intensity in air above a dry soil which is obtained from field calibration.

137

138 Field calibration at each site involved collection of gravimetric and volumetric soil samples at three distances
139 from the probe (25m, 100m and 200m) along each cardinal and inter-cardinal direction (i.e. 8 radial directions).
140 At each sample point, soil cores were taken to calculate volumetric soil moisture content for three depths (0 to 5
141 cm, 10 to 15 cm, and 25 to 30 cm), giving a total of 72 samples per calibration. Water content from samples was
142 determined by drying samples at 105°C for 24 hours (Klute, 1986). The depth weighted soil moisture from field
143 calibration was calculated using the method proposed by (Franz et al., 2012) and corresponding corrected
144 neutron count is used to determine N_0 in Eq. 5. Hydrogen held within the lattice structure of the soil minerals



145 and organic material can also effect neutron count rate and, hence, need to be considered in calculation
146 procedures. Lattice water (w_{lat}) was determined from the amount of water released at 1000°C preceded by
147 drying at 105°C. Soil organic carbon was estimated by measuring total organic carbon in samples using Heanes
148 wet oxidation, method 6B1 in Rayment and Higginson (1992). Following Franz et al. (2013) and Bogen et al.
149 (2013), the organic carbon was assumed to be present as cellulose, $C_6H_{10}O_5$, and this was converted into an
150 equivalent amount of water (w_{SOM}) by multiplying measured soil organic carbon by 0.556, which is the ratio of
151 five times the molecular weight of water to the molecular weight of cellulose.

152 2.3 Rover system

153 The rover system is based around a set of 16 custom made tube capsules supplied by Hydroinnova
154 (Albuquerque, USA), which are similar to those used for the static cosmic-ray soil moisture tubes but larger.
155 The rover has a counting rate ~18 times that of a standard static sensor allowing for measurements to be made at
156 one minute intervals. For a volumetric soil moisture content of 10% a count rate of around 350 c min⁻¹ was
157 recorded. The set of 16 tubes is mounted in a trailer from which additional measurements of air temperature,
158 relative humidity, atmospheric pressure and location were also made. While mobile, the measurements from the
159 system were monitored in real-time on a screen in the cabin of the tow vehicle. A dash mounted camera was
160 also used to collect images at one minute intervals during the survey.

161
162 For this investigation a nested design of broad scale and intensive localised measurements was implemented.
163 The broad scale design included a survey over an area with dimensions of approximately 36 x 36 km which
164 encapsulated a single Soil Moisture Active Passive (SMAP) satellite pixel. Using typical counting rates for this
165 area and by targeting an output resolution for soil moisture of 9 x 9 km we calculated that the maximum driving
166 speed for this survey was 90 km h⁻¹. This provided a good density of measurement points for interpolation
167 purposes. The survey area and measurement points from the driving track are shown in Figure 2. The broad
168 scale surveys typically took 10 h to complete, involved over 600 measurements and the average speed travelled
169 was around 60 km h⁻¹. The intensive scale survey covered an area of approximately 10 x 10 km and was located
170 in the south eastern corner of the broad scale survey (Figure 2). In this survey a target resolution for soil
171 moisture of 1 x 1 km was used for which we calculated that the maximum driving speed should not exceed 30
172 km h⁻¹. Much of the driving for the intensive scale surveys was around field boundaries and on unsealed roads.
173 Intensive scale surveys also took approximately 10 h to complete with more than 600 measurement point being
174 collected. The average speed during these surveys was 20 km h⁻¹. Survey tracks were defined for both surveys
175 prior to undertaking measurement using maps of the local road network. These maps were loaded into GIS
176 software and were used to guide navigation on each survey run.

177
178 Procedures used for correcting static cosmic-ray neutron sensor counts (Eq. 1 to Eq. 4) were also applied to the
179 rover data. Continually varying elevation, location, pressure, temperature and humidity were used for these
180 calculations. Soil moisture was also calculated in the same way as for the static sensors (Eq. 5) but there was a
181 requirement for spatial information regarding bulk density, soil organic matter and lattice water content. The
182 Soil and Landscape Grid of Australia provides ~90 x ~90 m pixels of digital soil attributes including bulk
183 density (Viscarra Rossel et al., 2014a) and soil organic carbon (Viscarra Rossel et al., 2014c) at depths of 0-5



184 cm, 5-15 cm and 15-30 cm which are useful for applying to rover surveys. The Soil and Landscape Grid of
185 Australia does not provide any lattice water information but it does provide information on clay content
186 (Viscarra Rossel et al., 2014b) and others (Greacen, 1981; Avery et al., 2016) have shown that clay content is
187 often a good predictor of lattice water. As an additional part of this study we investigated whether such a
188 relationship existing for the soils in the study area. To do this we collected 36 samples for lattice water analysis;
189 this included 25 distributed samples in the broad scale survey area, 9 samples across the intensive scale survey
190 area and the 2 samples collected as part of the calibration of the static probes. These samples were from cores
191 extracted from 0-30 cm depth. The spatial maps of bulk density, clay content and organic carbon used in the
192 rover calculation procedures are shown in Figure 3, also shown for site characterisation is the digital elevation
193 model for the survey area.

194

195 Use of Eq. 5 in rover surveys also requires specification of a suitable N_0 value. For the static sensors this value
196 is derived through the calibration procedures. To calculate N_0 for the rover we undertook side-by-side
197 comparisons with the static sensors which involved parking next to a static sensor for 12 hours prior to a survey.
198 The average counts from the rover and static sensor were then compared to derive a suitable scaling approach to
199 derive a rover-specific N_0 . Both broad scale and intensive scale surveys were undertaken on three separate
200 occasions on consecutive days during April 2016, June 2016 and March 2017.

201

202 Interpolation of the rover count data was required to produce a spatial representation of count rates for the entire
203 survey area. To achieve this the Variogram Estimation and Spatial Prediction with Error (VESPER) software
204 package (Minasny et al., 2005) was used. VESPER was used to undertake conventional kriging with a global
205 variogram. An exponential variogram model was used for both survey scales and an interpolated grid of
206 corrected rover count rate was produced at 90 m resolution to match that of the underlying soils information.

207 **3 Results**

208 **3.1 Static CRNS calibration**

209 Prior to deployment, the two static sensors were run side-by-side for a period of 4 days to determine if there
210 were any differences in counting rates that were not attributable to local conditions. Over this period the average
211 counting rate differed by less than 1%, thus giving confidence that differences between sensors reflect local site
212 characteristics alone. Calibration of the two CRNS occurred under different soil moisture conditions; at Bennetts
213 the depth weighted soil moisture content was $0.13 \text{ m}^3 \text{ m}^{-3}$, while at Bishes it was $0.08 \text{ m}^3 \text{ m}^{-3}$. Fitting of the
214 calibration curve to these two sites resulted in remarkable similarity in derived dry soil (N_0) counting rates with
215 analysis of the data collected at Bennetts producing an N_0 of 1541 c h^{-1} and that from Bishes producing an N_0 of
216 1583 c h^{-1} . These differences are very small and reflect the fact that hydrogen represented by the biomass pool is
217 basically non-existent at these sites.



218 3.2 Rover calibration

219 Calibration of the rover was undertaken through side-by-side comparison with the Bennetts CRNS and the
220 Bishes CRNS on two separate occasions each. These comparisons covered a range of soil moisture conditions
221 over four separate 12 h periods. Table 1 shows the corresponding neutron count rate for the rover and each
222 CRNS and the scaling factor that converts static CRNS counting rate to a rover equivalent; this scaling factor is
223 used to scale the N_0 values derived for each static sensor to an equivalent N_0 for the rover. Despite the
224 differences in conditions and site characteristics, the scaling factor remained relatively constant, as did the
225 derived N_0 for each comparison period. Given the relatively constant relationship between the rover and static
226 sensors an average N_0 of 460 c min⁻¹ was derived and this value was applied across all surveys.

227 3.3 Spatial lattice water information

228 The volumetric soil moisture equation for cosmic-ray soil moisture measurements (Eq. 5) requires information
229 on soil organic matter content, bulk density and lattice water. For our rover surveys spatial data sets exist for
230 organic matter and bulk density but not for lattice water. A relationship between clay content and lattice water
231 content has been noted by others therefore samples were collected to test for similar relationships across our
232 survey area. A comparison of clay content and lattice water content for 36 spatially distributed samples shows a
233 strong linear relationship ($R^2 = 0.7$) across a broad range of clay content (4–56%). This relationship was applied
234 to the spatial clay content data set from the Soil and Landscape Grid of Australia (Viscarra Rossel et al., 2014b)
235 to produce an equivalent lattice water dataset at 90 m resolution.

236 3.4 Spatial estimation

237 Example variograms from the kriging procedures used for broad scale and intensive surveys are shown in Figure
238 6. Both surveys utilise exponential variogram models however the fit is different with the intensive scale
239 surveys having a distinct ‘sill’ and broad scale variograms showing no ‘sill’ at all. The variogram model for the
240 intensive surveys showed more cyclicity (or ‘hole effect’) which could be related to underlying geological
241 periodicity (Yang and Kaleita, 2007). The empirical variograms were well described by the exponential models
242 giving confidence in interpolated rover counts across the respective survey areas.

243 3.5 Intensive scale rover surveys

244 Interpolated counts and derived volumetric soil moisture content for each of the three intensive scale surveys is
245 shown in Figure 7. A large range in soil moisture content was observed over the three surveys with values
246 ranging between 0.01 m³ m⁻³ in April 2016 through to 0.30 m³ m⁻³ in June 16. Higher than average counting
247 rates and, hence, lower soil moisture were consistently observed in the central northern region of the survey
248 area. This area is characterised by a ridge of sandy soil with rock fragments and is known locally as ‘Sandhill’.
249 Wetter soil moisture conditions were observed through the central and southern parts of the survey area. We
250 note here that although the data are presented at 90 m resolution this is due to calculations being undertaken at
251 the scale of the underlying soil grid; the intended output of this survey is a 1 x 1 km soil moisture product.

252



253 Comparison of intensive rover survey soil moisture estimates for the CRNS locations at the three different
254 survey dates shows excellent agreement between the two measurement methods (Figure 8). The rover survey
255 estimate is taken from the 1 km resolution soil moisture estimate for the corresponding CRNS pixel.
256 Comparisons of estimates for the Bennetts CRNS shows differences of less than $0.025 \text{ m}^3 \text{ m}^{-3}$ for all three
257 occasions. The rover survey estimates tended to underestimate the soil moisture measured at the Bishes CRNS.
258 The largest difference was during the April 2016 survey where soil moisture was underestimated by $0.04 \text{ m}^3 \text{ m}^{-3}$.
259 It is possible that this underestimation is a result of local interpolation issues. The Bishes CRNS is in close
260 proximity to the sandy ridge known as ‘Sandhill’ which represents a distinct zone of low soil moisture (Figure
261 7). The effect of this abrupt change is likely to be ‘smoothed’ within the area that also encompasses the Bishes
262 CRNS.
263
264 The rover surveys at the intensive scale also offer the opportunity to estimate soil moisture at the farm property
265 scale. A number of properties in the intensive scale zone are identified in Figure 9 and the intensive scale rover
266 survey from March 2017 has been used to derive property average soil moisture conditions. The average size of
267 the identified properties is approximately 1 km^2 . As well as enabling direct estimates at the time of the surveys
268 there is also the opportunity to combine property average soil moisture content at the survey times and CRNS
269 observations in a regression analysis approach to derive a much higher time resolution soil moisture product at
270 the property scale. This approach assumes that rainfall is relatively uniform across the region and that crops are
271 planted across all periods; both of which are typical in this study area. Regression relationships were developed
272 between the Bennetts CRNS and 50 properties in the intensive survey area (see Table A1). Point-to-area
273 regression analysis showed very strong linear relationships with an average R^2 value of 0.97 (range = 0.87-1.00).
274 Application of these regression models to derive time-series of property scale soil moisture for three example
275 properties is given in Figure 10. We note that the opportunity also exists to use similar point-to-area scaling
276 techniques to derive high temporal resolution soil moisture products at other set resolutions (e.g. 1 km) which
277 would make for ideal datasets for testing model and satellite soil moisture estimates.
278

279 3.6 Broad scale rover surveys

280 Interpolated counts and derived volumetric soil moisture content for each of the three broad scale surveys is
281 shown in Figure 11. The common feature of all of the survey dates is the tendency for higher counts and, hence,
282 lower soil moisture to occur at the north-western region of the survey area and lower counts and, hence higher
283 soil moisture to occur in the south-eastern region. These patterns reflect soil textures in the region with sandier
284 soils and dunes with low clay content in the north-western and higher clay content soils in south-east. The driest
285 soil moisture conditions were experienced during the April 2016 survey with a mean soil moisture of $0.05 \text{ m}^3 \text{ m}^{-3}$
286 (range = $0.01\text{--}0.10 \text{ m}^3 \text{ m}^{-3}$) and the wettest were observed during the June 2016 survey with a mean soil
287 moisture of $0.17 \text{ m}^3 \text{ m}^{-3}$ (range = $0.09\text{--}0.27 \text{ m}^3 \text{ m}^{-3}$). The March 2017 survey provided intermediate soil
288 moisture conditions with a mean for the region of $0.09 \text{ m}^3 \text{ m}^{-3}$ (range = $0.04\text{--}0.15 \text{ m}^3 \text{ m}^{-3}$).
289
290 The nested design of the intensive and broad scale surveys (Figure 2) enables the accuracy of broad scale survey
291 estimates to be assessed. To undertake such an analysis, we selected a $9 \times 9 \text{ km}$ region within the area of survey



292 overlap (Figure 2) and derived corresponding soil moisture estimates at resolutions of 1, 3 and 9 km. The
293 intensive survey results can be considered as a point of truth for broad survey results. The difference in soil
294 moisture estimates between the broad and intensive scale surveys for different resolutions on each of the three
295 survey dates is shown in Figure 12. The broad scale survey estimates are clearly not a good representation of 1 x
296 1 km scale soil moisture as survey speeds and sampling points are not detailed enough to pick up local soil
297 moisture variations. Differences of up to $\pm 0.10 \text{ m}^3 \text{ m}^{-3}$ were observed. At 3 x 3 km resolution the performance of
298 the broad scale survey estimates improves but there are still some distinct zones where soil moisture differed by
299 as much as $\pm 0.06 \text{ m}^3 \text{ m}^{-3}$. At the 9 x 9 km scale, for which the broad scale surveys were designed, differences in
300 soil moisture between the intensive and broad scale surveys was minimal. On all three occasions the difference
301 was less than $0.005 \text{ m}^3 \text{ m}^{-3}$. These comparisons validate our broad scale experimental design and give
302 confidence in the 9 x 9 km resolution soil moisture produced from our rover surveys.

303 4 Discussion

304 Static CRNS calibration at Bishes and Bennetts produced very similar dry soil counting rate (N_0). This
305 similarity has resulted because hydrogen in soil water, lattice water and organic matter is accounted for in the
306 calibration process and because both sites are devoid of above ground biomass. The effect of biomass on N_0 has
307 been noted by Hawdon et al. (2014) who compared N_0 values from eight probes from across the Australian
308 CRNS network with site biomass and also by Baatz et al. (2015) who proposed an empirical biomass correction
309 for CRNS calibration. This finding has important implications for rover surveys in this region as the landscape
310 in the Mallee region is almost entirely cleared of forest and above ground biomass is represented by pasture and
311 crop cover. McJannet et al. (2014) calculated that pasture represented a biomass water equivalent of just 0.6
312 mm a value similar to that derived by Baatz et al. (2015) for areas dominated by crops; these small values show
313 that these small hydrogen pools will have little impact on neutron counts (McJannet et al., 2014).

314

315 In this present study the N_0 value for converting rover neutron counting rates to soil moisture content was
316 derived through side by side comparison with the two CRNS sensors. A similar approach was employed by
317 Chrisman and Zreda (2013) using a single CRNS as a reference point and by Dong et al. (2014) using a network
318 of in situ measurements. Rover surveys undertaken by Franz et al. (2015) also used comparison with static
319 CRNS sensors but in their investigations a further correction was introduced to account for variations in above
320 ground biomass. Locations with greater biomass should adopt a calibration schemes that include this hydrogen
321 pool (i.e. Baatz et al., 2015; Franz et al., 2013).

322

323 Rover surveys require information on the spatial variation in bulk density, soil organic matter and lattice water
324 for calculation of soil moisture content using conventional approaches. While pre-existing bulk density and
325 organic matter datasets exist for Australia we had to derive a lattice water dataset based on a strong region-wide
326 relationship with clay content. The relationship we derived for the study area was different to that proposed by
327 Greacen (1981) for Australian soils and may reflect differences in the soil types included in the analysis. With
328 the intent of producing a similar spatial lattice water dataset for the continental United States, Avery et al.



329 (2016) derived relationships with clay content but found that relationships were weak for many soil taxonomic
330 group. For best local results a spatial sampling such as that utilised in this present study is recommended.
331 A factor that has not been accounted for in our rover surveys is the potential impacts of roads on our survey
332 results. By design roads will have a low moisture content and the impact of this narrow strip within the sensor
333 footprint on survey results has not yet been accounted for in rover studies reported in the literature. Using
334 neutron modelling approaches Köhli et al. (2015) demonstrated that a CRNS is most sensitive to soil moisture in
335 the nearest tens of metres and showed that dry roads can contribute to an over estimate of neutron counts by a
336 few percent. In the survey areas in which our broad scale rover surveys were undertaken more than 70% of the
337 roads were unsealed and many of the sealed roads were only one lane wide; while this does not remove the issue
338 it does lessen the potential impact on reported results considerably. The impact of roads on our intensive scale
339 surveys is likely to be even less as 60% of the observations were made while driving around property
340 boundaries (i.e. not properly formed roads) and a further 30% were on unsealed roads. While the impact of
341 roads may not be a major issue for the present study it is an issue that needs some warrants consideration in
342 future surveys.

343

344 Intensive scale surveys were designed to produce a 1 x 1 km resolution soil moisture product and comparison to
345 static CRNS observations supports this. Detailed soil moisture maps highlight the impact that soil properties
346 have on observed soil moisture with sandier locations being typically drier when compared to those with more
347 clay. Property scale soil moisture estimates led to the development of point-to-area style regression models
348 which then enabled continuous estimates of soil moisture to be made at the property scale. The regression
349 modelling showed that temporal patterns in soil moisture were strong. Similar observations have been reported
350 for other studies (Kachanoski and Jong, 1988; Grayson and Western, 1998; Vachaud et al., 1985). According to
351 Yang and Kaleita (2007) spatial patterns of soil moisture exhibit some degree of temporal stability which is
352 related to time invariant attributes such as topography and soil characteristics. With the relatively flat
353 topography in Mallee study area and the assumption that rainfall inputs and crop growth are similar between
354 properties, it is likely that differences in the slopes and intercepts of relationship between CRNS observations
355 and property scale soil moisture (see Table A1) are being controlled by local soil characteristics. Changes in
356 local crops and local scale differences in rainfall inputs (i.e. small convective storms) do of course have the
357 potential to change these point-to-area relationships but if these factors can be accounted for then useful spatial
358 and temporal soil moisture datasets can be produced.

359

360 Broad scale surveys produced reliable soil moisture estimates at 9 x 9 km resolution although the faster survey
361 speeds and lower measurement density meant that this survey was unable to distinguish many of the smaller
362 scale soil moisture variations revealed at the finer resolution and slower survey speeds of the intensive scale
363 survey. This clearly supports the need to design rover surveys for the scale of analysis to be eventually
364 undertaken.



365 **5 Conclusion**

366 In this study we presented an investigation designed to produce soil moisture estimates across a range of scales.
367 Our investigation involved static CRNS sensors and rover surveys at both broad and intensive scales. We
368 established techniques for converting neutron counting rates from the rover to soil moisture using side-by-side
369 comparisons with static CRNS sensors and spatial datasets of soil characteristics. In particular we found that
370 lattice water was strongly related to clay content in the study area and used this relationship to derive a spatial
371 representation of lattice water.

372
373 Rover surveys were undertaken across soils ranging in moisture content from 0.01 to 0.30 m³ m⁻³ and reliable
374 results were produced across all conditions. The slower driving speeds and denser sampling network of the
375 intensive surveys provided representation of local soil moisture variations at resolutions down to 1 x 1 km.
376 Stability in observed spatial patterns of soil moisture were used in a regression modelling approach to produce
377 time series of property scale soil moisture based on CRNS observations. Broad scale surveys, which
378 incorporated higher driving speeds and sparser sampling points, were shown to produce excellent
379 representations of soil moisture at 9 x 9 km pixel resolution making them well suited for assessing variation in
380 this parameter at a regional scale. The multiscale application of the rover makes it a unique tool for addressing
381 soil moisture questions across scales previously not possible. The multiscale soil moisture products produced in
382 this study are well suited to future analysis of both satellite soil moisture retrievals and finer scale soil moisture
383 models.

384

385 **Acknowledgements**

386 The authors acknowledge the cooperation of Tim McClelland and family who allowed access to their properties
387 for installations and surveys. We are grateful to staff from the Birchip Cropping Group who helped with
388 surveys and sample analysis. Several anonymous reviewers and Auro Almeida are thanked for their valuable
389 comments. Funding for this research was provided by the Department of Agriculture & Water (Grant
390 Agreement GMS-2582) and CSIRO. We acknowledge the NMDB database (www.nmdb.eu), founded under the
391 European Union's FP7 programme (contract no. 213007) for providing neutron monitor data. Lomnický
392 štít neutron monitor data (LMKS) were kindly provided by the Department of Space Physics, Institute of
393 Experimental Physics, Košice, Slovakia.

394

395

396 **References**

397

398 Anwar, M. R., O'Leary, G., McNeil, D., Hossain, H., and Nelson, R.: Climate change impact on rainfed wheat
399 in south-eastern Australia, *Field Crops Research*, 104, 139-147, 10.1016/j.fcr.2007.03.020, 2007.400 Avery, W. A., Finkenbiner, C., Franz, T. E., Wang, T., Nguy-Robertson, A. L., Suyker, A., Arkebauer, T., and
401 Muñoz-Arriola, F.: Incorporation of globally available datasets into the roving cosmic-ray neutron probe method
402 for estimating field-scale soil water content, *Hydrol. Earth Syst. Sci.*, 20, 3859-3872, 10.5194/hess-20-3859-
403 2016, 2016.404 Baatz, R., Bogaen, H. R., Hendricks Franssen, H. J., Huisman, J. A., Qu, W., Montzka, C., and Vereecken, H.:
405 Calibration of a catchment scale cosmic-ray probe network: A comparison of three parameterization methods, *J.*
406 *Hydrol.*, 516, 231-244, 10.1016/j.jhydrol.2014.02.026, 2014.407 Baatz, R., Bogaen, H. R., Hendricks Franssen, H. J., Huisman, J. A., Montzka, C., and Vereecken, H.: An
408 empirical vegetation correction for soil water content quantification using cosmic ray probes, *Water Resour.*
409 *Res.*, 2030-2046, 10.1002/2014wr016443, 2015.410 Bogaen, H. R., Herbst, M., Huisman, J. A., Rosenbaum, U., Weuthen, A., and Vereecken, H.: Potential of
411 Wireless Sensor Networks for Measuring Soil Water Content Variability All rights reserved. No part of this
412 periodical may be reproduced or transmitted in any form or by any means, electronic or mechanical, including
413 photocopying, recording, or any information storage and retrieval system, without permission in writing from
414 the publisher, *Vadose Zone Journal*, 9, 1002-1013, 10.2136/vzj2009.0173, 2010.415 Bogaen, H. R., Huisman, J. A., Baatz, R., Hendricks Franssen, H. J., and Vereecken, H.: Accuracy of the
416 cosmic-ray soil water content probe in humid forest ecosystems: The worst case scenario, *Water Resour. Res.*,
417 49, 5778-5791, 10.1002/wrcr.20463, 2013.418 Chrisman, B., and Zreda, M.: Quantifying mesoscale soil moisture with the cosmic-ray rover, *Hydrol. Earth*
419 *Syst. Sci.*, 17, 5097-5108, 10.5194/hess-17-5097-2013, 2013.420 Desilets, D., and Zreda, M.: Spatial and temporal distribution of secondary cosmic-ray nucleon intensities and
421 applications to in situ cosmogenic dating, *Earth Planet. Sci. Lett.*, 206, 21-42, 10.1016/s0012-821x(02)01088-9,
422 2003.423 Desilets, D., Zreda, M., and Prabu, T.: Extended scaling factors for in situ cosmogenic nuclides: New
424 measurements at low latitude, *Earth Planet. Sci. Lett.*, 246, 265-276, 10.1016/j.epsl.2006.03.051, 2006.425 Desilets, D., Zreda, M., and Ferre, T. P. A.: Nature's neutron probe: Land surface hydrology at an elusive scale
426 with cosmic rays, *Water Resour. Res.*, 46, 10.1029/2009wr008726, 2010.427 Desilets, D., and Zreda, M.: Footprint diameter for a cosmic-ray soil moisture probe: Theory and Monte Carlo
428 simulations, *Water Resour. Res.*, 49, 3566-3575, 10.1002/wrcr.20187, 2013.429 Dong, J., Ochsner, T. E., Zreda, M., Cosh, M. H., and Zou, C. B.: Calibration and Validation of the COSMOS
430 Rover for Surface Soil Moisture Measurement, *Vadose Zone Journal*, 13, 10.2136/vzj2013.08.0148, 2014.431 Evans, J. G., Ward, H. C., Blake, J. R., Hewitt, E. J., Morrison, R., Fry, M., Ball, L. A., Doughty, L. C., Libre, J.
432 W., Hitt, O. E., Rylett, D., Ellis, R. J., Warwick, A. C., Brooks, M., Parkes, M. A., Wright, G. M. H., Singer, A.
433 C., Boorman, D. B., and Jenkins, A.: Soil water content in southern England derived from a cosmic-ray soil
434 moisture observing system – COSMOS-UK, *Hydrological Processes*, 30, 4987-4999, 10.1002/hyp.10929, 2016.435 Franz, T. E., Zreda, M., Ferre, T. P. A., Rosolem, R., Zweck, C., Stillman, S., Zeng, X., and Shuttleworth, W. J.:
436 Measurement depth of the cosmic ray soil moisture probe affected by hydrogen from various sources, *Water*
437 *Resour. Res.*, 48, W08515, 10.1029/2012wr011871, 2012.438 Franz, T. E., Zreda, M., Rosolem, R., and Ferre, T. P. A.: A universal calibration function for determination of
439 soil moisture with cosmic-ray neutrons, *Hydrol. Earth Syst. Sci.*, 17, 453-460, 10.5194/hess-17-453-2013, 2013.



- 440 Franz, T. E., Wang, T., Avery, W., Finkenbinder, C., and Brocca, L.: Combined analysis of soil moisture
441 measurements from roving and fixed cosmic ray neutron probes for multiscale real-time monitoring, *Geophys.*
442 *Res. Lett.*, 1-8, 10.1002/2015gl063963, 2015.
- 443 Grayson, R. B., and Western, A. W.: Towards areal estimation of soil water content from point measurements:
444 time and space stability of mean response, *J. Hydrol.*, 207, 68-82, 1998.
- 445 Greacen, E. L.: Soil water assessment by the neutron method, in, edited by: Greacen, G. L., *Soil water*
446 *assessment by the neutron method*, CSIRO Australia, Adelaide, 1981.
- 447 Hawdon, A., McJannet, D., and Wallace, J.: Calibration and correction procedures for cosmic-ray neutron soil
448 moisture probes located across Australia, *Water Resour. Res.*, 50, 5029-5043, 10.1002/2013wr015138, 2014.
- 449 Holgate, C. M., De Jeu, R. A. M., van Dijk, A. I. J. M., Liu, Y. Y., Renzullo, L. J., Vinodkumar, Dharssi, I.,
450 Parinussa, R. M., Van Der Schalie, R., Gevaert, A., Walker, J., McJannet, D., Cleverly, J., Haverd, V.,
451 Trudinger, C. M., and Briggs, P. R.: Comparison of remotely sensed and modelled soil moisture data sets
452 across Australia, *Remote Sensing of Environment*, 186, 479-500, <http://dx.doi.org/10.1016/j.rse.2016.09.015>,
453 2016.
- 454 Kachanoski, R., and Jong, E.: Scale dependence and the temporal persistence of spatial patterns of soil water
455 storage, *Water Resour. Res.*, 24, 85-91, 1988.
- 456 Kędzior, M., and Zawadzki, J.: Comparative study of soil moisture estimations from SMOS satellite mission,
457 GLDAS database, and cosmic-ray neutrons measurements at COSMOS station in Eastern Poland, *Geoderma*,
458 283, 21-31, <http://dx.doi.org/10.1016/j.geoderma.2016.07.023>, 2016.
- 459 Klute, A.: *Methods of soil analysis. Part 1. Physical and mineralogical methods*, American Society of
460 Agronomy, Inc., 1986.
- 461 Köhli, M., Schrön, M., Zreda, M., Schmidt, U., Dietrich, P., and Zacharias, S.: Footprint characteristics revised
462 for field-scale soil moisture monitoring with cosmic-ray neutrons, *Water Resour. Res.*, 51, 5772-5790,
463 10.1002/2015wr017169, 2015.
- 464 McJannet, D., Franz, T., Hawdon, A., Boadle, D., Baker, B., Almeida, A., Silberstein, R., Lambert, T., and
465 Desilets, D.: Field testing of the universal calibration function for determination of soil moisture with cosmic-
466 ray neutrons, *Water Resour. Res.*, 50, 5235-5248, 10.1002/2014wr015513, 2014.
- 467 Minasny, B., McBratney, A. B., and Whelan, B. M.: *VESPER version 1.62*, The University of Sydney, NSW
468 2006, Australian Centre for Precision Agriculture, 2005.
- 469 Montzka, C., Bogena, H., Zreda, M., Monerris, A., Morrison, R., Muddu, S., and Vereecken, H.: Validation of
470 Spaceborne and Modelled Surface Soil Moisture Products with Cosmic-Ray Neutron Probes, *Remote Sensing*,
471 9, 103, 2017.
- 472 NASA: *US standard atmosphere, 1976*, NOAA-S/T, 1976.
- 473 Ochsner, T. E., Cosh, M. H., Cuenca, R. H., Dorigo, W. A., Draper, C. S., Hagimoto, Y., Kerr, Y. H., Njoku, E.
474 G., Small, E. E., and Zreda, M.: State of the Art in Large-Scale Soil Moisture Monitoring, *Soil Sci. Soc. Am. J.*,
475 77, 1888-1919, 10.2136/sssaj2013.03.0093, 2013.
- 476 Rayment, G. E., and Higginson, F. R.: *Australian laboratory handbook of soil and water chemical methods*,
477 Inkata Press Pty Ltd, 1992.
- 478 Renzullo, L. J., van Dijk, A. I. J. M., Perraud, J. M., Collins, D., Henderson, B., Jin, H., Smith, A. B., and
479 McJannet, D. L.: Continental satellite soil moisture data assimilation improves root-zone moisture analysis for
480 water resources assessment, *J. Hydrol.*, 519, 3338-3352, <http://dx.doi.org/10.1016/j.jhydrol.2014.08.008>, 2014.



- 481 Rosolem, R., Shuttleworth, W. J., Zreda, M., Franz, T. E., Zeng, X., and Kurc, S. A.: The Effect of Atmospheric
482 Water Vapor on Neutron Count in the Cosmic-Ray Soil Moisture Observing System, *Journal of*
483 *Hydrometeorology*, 10.1175/jhm-d-12-0120.1, 2013.
- 484 Smith, A. B., Walker, J. P., Western, A. W., Young, R. I., Ellett, K. M., Pipunic, R. C., Grayson, R. B.,
485 Siriwardena, L., Chiew, F. H. S., and Richter, H.: The Murrumbidgee soil moisture monitoring network data set,
486 *Water Resour. Res.*, 48, W07701, 10.1029/2012WR011976, 2012.
- 487 Vachaud, G., Passerat de Silans, A., Balabanis, P., and Vauclin, M.: Temporal stability of spatially measured
488 soil water probability density function, *Soil Sci. Soc. Am. J.*, 49, 822-828, 1985.
- 489 Vereecken, H., Huisman, J. A., Pachepsky, Y., Montzka, C., van der Kruk, J., Bogaen, H., Weiermüller, L.,
490 Herbst, M., Martinez, G., and Vanderborght, J.: On the spatio-temporal dynamics of soil moisture at the field
491 scale, *J. Hydrol.*, 516, 76-96, 10.1016/j.jhydrol.2013.11.061, 2014.
- 492 Vinodkumar, Dharssi, I., Bally, J., Steinle, P., McJannet, D., and Walker, J.: Comparison of soil wetness from
493 multiple models over Australia with observations, *Water Resour. Res.*, 1-14, 10.1002/2015wr017738, 2017.
- 494 Viscarra Rossel, R., Chen, C., Grundy, M., Searle, R., Clifford, D., Odgers, N., Holmes, K., Griffin, T.,
495 Liddicoat, C., and Kidd, D.: Soil and Landscape Grid National Soil Attribute Maps - Bulk Density - Whole
496 Earth (3" resolution) - Release 1. v4, CSIRO Data Collection. <http://doi.org/10.4225/08/546EE212B0048>,
497 2014a.
- 498 Viscarra Rossel, R., Chen, C., Grundy, M., Searle, R., Clifford, D., Odgers, N., Holmes, K., Griffin, T.,
499 Liddicoat, C., and Kidd, D.: Soil and Landscape Grid National Soil Attribute Maps - Clay (3" resolution) -
500 Release 1. v4, CSIRO Data Collection. <http://doi.org/10.4225/08/546EEE35164BF>, 2014b.
- 501 Viscarra Rossel, R., Chen, C., Grundy, M., Searle, R., Clifford, D., Odgers, N., Holmes, K., Griffin, T.,
502 Liddicoat, C., and Kidd, D.: Soil and Landscape Grid National Soil Attribute Maps - Organic Carbon (3"
503 resolution) - Release 1. v1., CSIRO Data Collection. <http://doi.org/10.4225/08/547523BB0801A>, 2014c.
- 504 Western, A. W., and Blöschl, G.: On the spatial scaling of soil moisture, *J. Hydrol.*, 217, 203-224,
505 10.1016/S0022-1694(98)00232-7, 1999.
- 506 Yang, L., and Kaleita, A. L.: *Understanding Spatio-temporal Patterns of Soil Moisture at the Field Scale*, 2007.
- 507 Zreda, M., Desilets, D., Ferre, T. P. A., and Scott, R. L.: Measuring soil moisture content non-invasively at
508 intermediate spatial scale using cosmic-ray neutrons, *Geophys. Res. Lett.*, 35, L21402 10.1029/2008gl035655,
509 2008.
- 510 Zreda, M., Shuttleworth, W. J., Zeng, X., Zweck, C., Desilets, D., Franz, T., and Rosolem, R.: COSMOS: the
511 COsmic-ray Soil Moisture Observing System, *Hydrol. Earth Syst. Sci.*, 16, 4079-4099, 10.5194/hess-16-4079-
512 2012, 2012.
- 513
- 514



515 **6 Tables and captions**

516

517 **Table 1. Side-by-side comparison of average neutron counts for the static CRNS's (Bishes and Bennetts) and the**
 518 **rover for 4 different 12 hour periods. Also shown are the static CRP to rover scaling factors and derived dry soil**
 519 **counting rate, N_0 , for the rover. All counts are in c min^{-1} for application to rover data.**

Date	Site	Static CRNS average counts (c min^{-1})	Rover average counts (c min^{-1})	Static to rover scaling factor	Static CRNS N_0 (c min^{-1})	Derived rover N_0 (c min^{-1})
10 April 2016	Bishes	21.74	370.0	17.0	26.4	449
1 March 2017	Bishes	20.4	364.8	17.9	26.4	471
9 June 2016	Bennetts	15.23	268.1	17.6	25.7	452
2 March 2017	Bennetts	16.8	307.6	16.8	25.7	469
			Average	17.3	Average	460

520

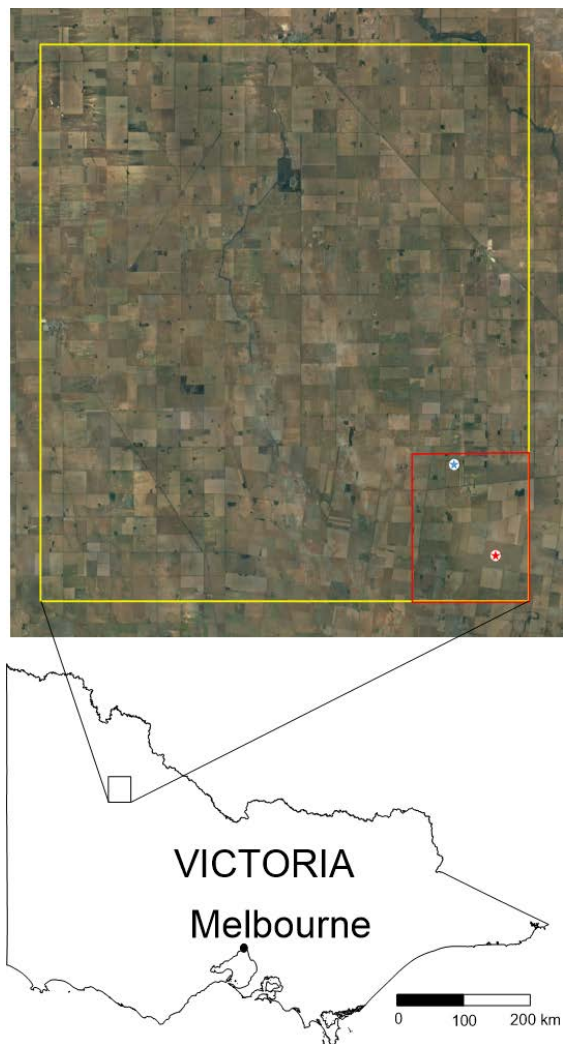
521

522



523 7 Figures and captions

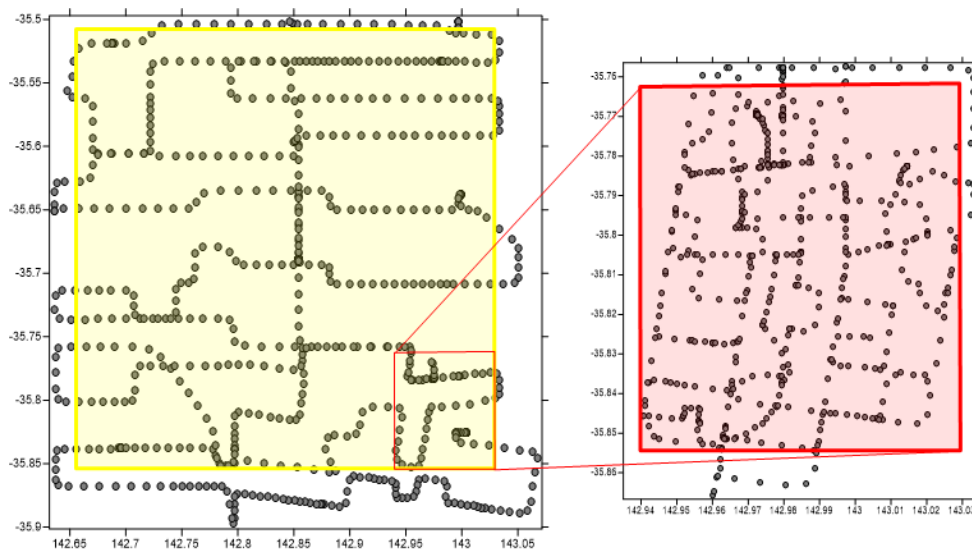
524



525

526 **Figure 1.** Location of field site in western Victoria, Australia. Yellow rectangle shows extent of broad scale rover
527 surveys and red rectangle shows extent of intensive surveys. Blue and red stars indicate the location of the Bishes and
528 Bennetts cosmic-ray soil moisture sensors. Imagery data: Google, TerraMetrics 2017.

529



530

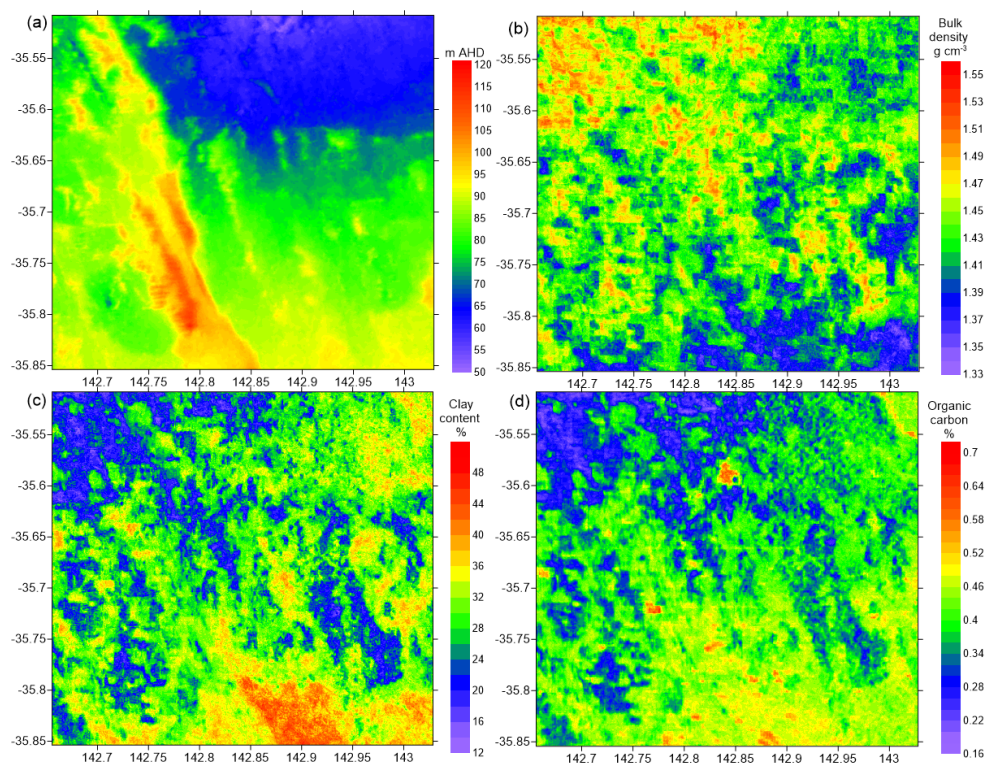
531

532

533

Figure 2. Rover survey extents and sampling points for the broad scale and intensive scale measurement campaigns. Sampling points from April 2016. The yellow box (~36km x 36km) delineates the broad scale survey extent and the red box (~10km x 10 km) delineates the intensive scale survey extent.

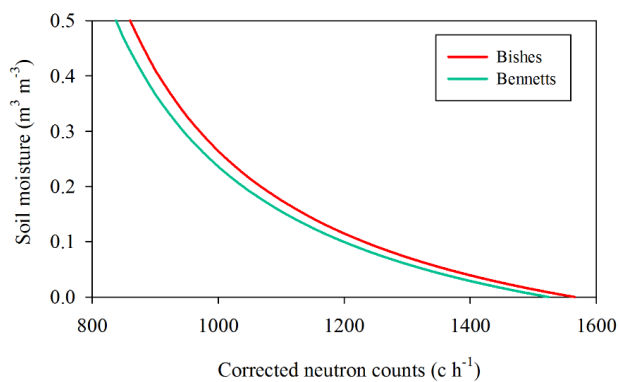
534



535

536 **Figure 3. Field survey area DEM (a), depth weighted 0–30 cm bulk density (b), depth weighted 0–30 cm clay content**
537 **(c), and depth weighted 0–30 cm organic matter content (d).**

538

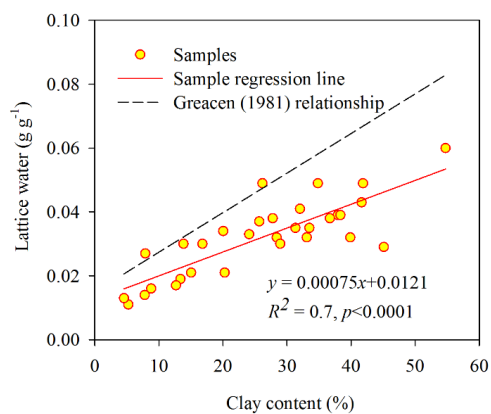


539

540 **Figure 4. Calibration curves for converting corrected neutron counts to soil moisture content for the Bishes and**
541 **Bennetts cosmic ray soil moisture sensors. The dry soil counting rate, N_0 , is 1583 c h⁻¹ for Bishes and 1541 c h⁻¹ for**
542 **Bennetts.**

543

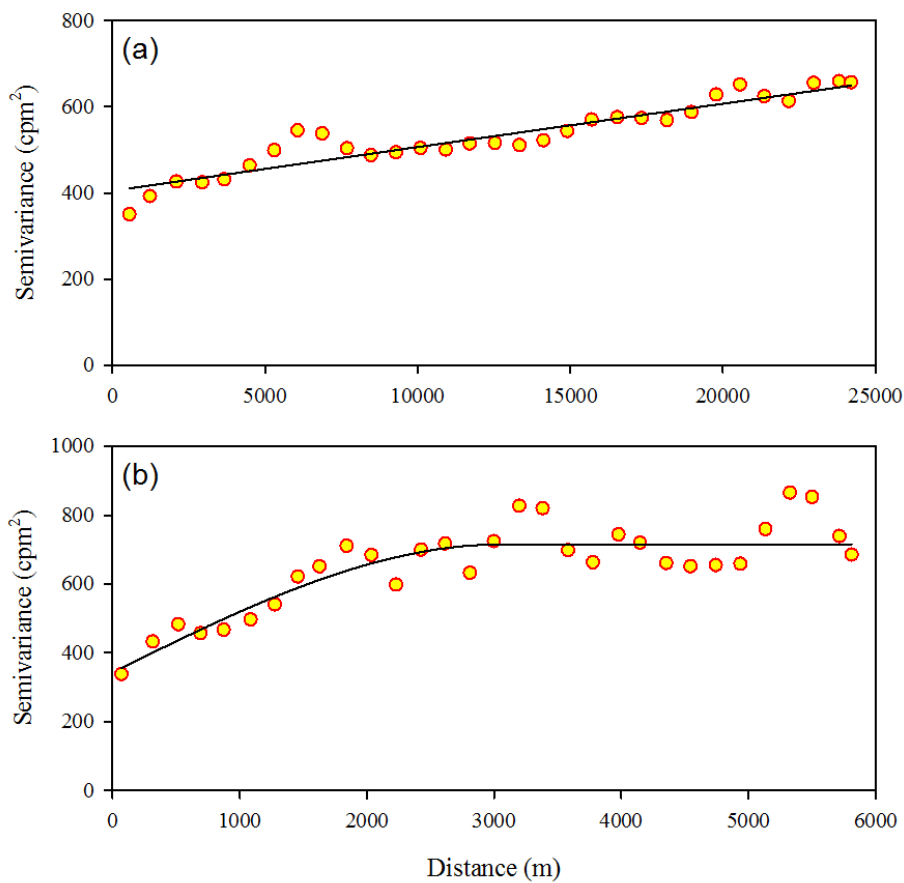
544



545

546 **Figure 5. Clay content vs Lattice water showing sample points from the study area and fitted relationship. Also**
547 **shown for reference is the relationship proposed by Greacen (1981).**

548

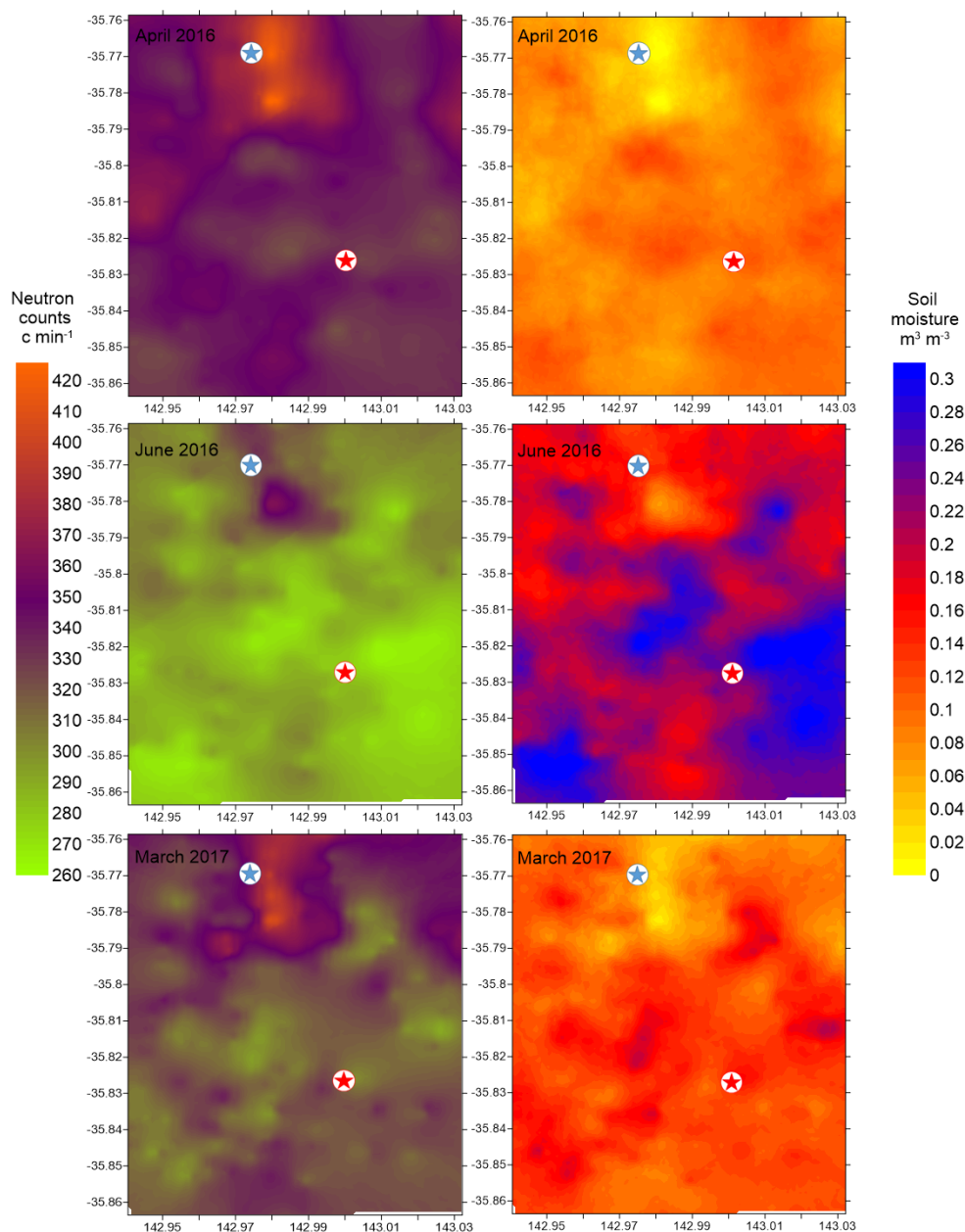


549

550 **Figure 6. Example variograms used for block kriging for broad scale and intensive surveys. The broad scale**
551 **variogram is from April 2016 (a) and the intensive scale variogram is from June 2016 (b).**

552

553

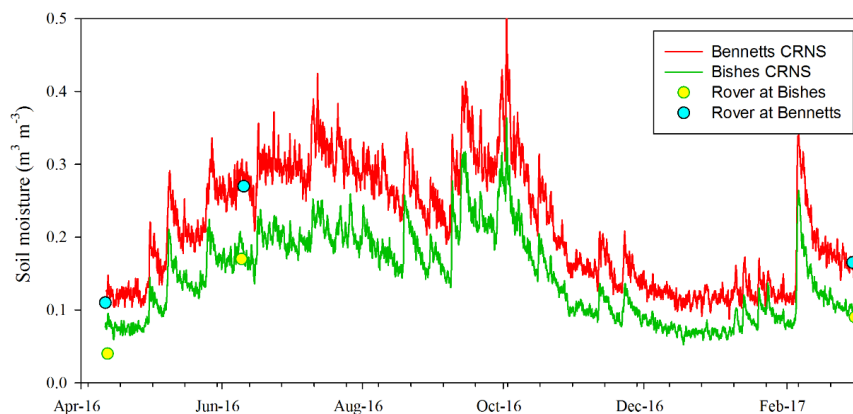


554

555 **Figure 7. Interpolated counts (left column) and derived soil moisture (right column) for the three intensive scale**
556 **surveys during April 2016, June 2016 and March 2017. Blue and red stars indicate the location of the Bishes and**
557 **Bennetts cosmic-ray soil moisture sensors.**

558

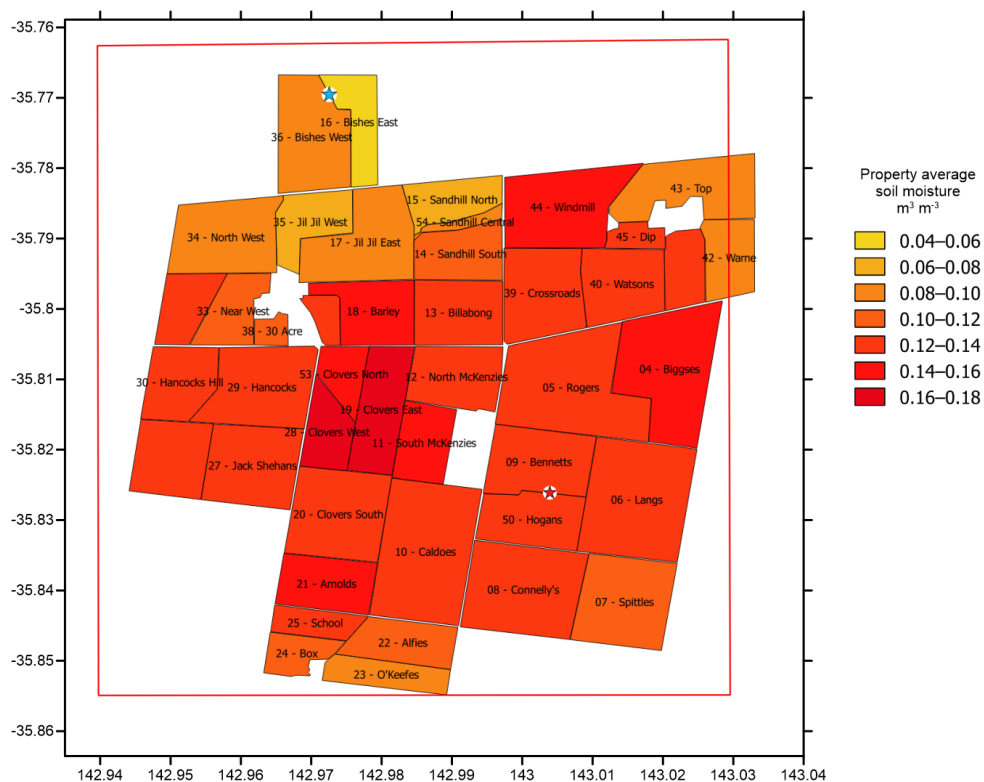
559



560

561 **Figure 8. Comparison of Bennetts and Bishes CRNS soil moisture estimates and corresponding intensive rover survey**
562 **estimates for the CRNS locations for the three survey dates. Rover survey estimate is from 1 km resolution pixel**
563 **corresponding to each CRNS location.**

564



565

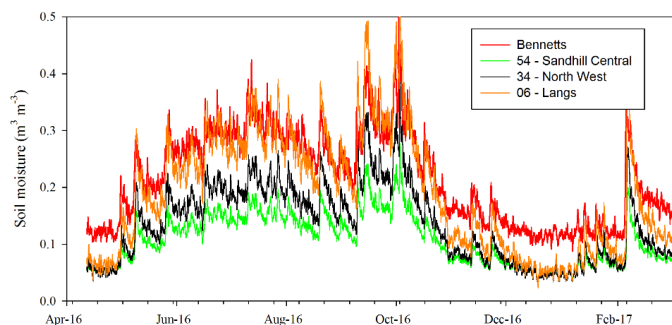
566

567

568

569

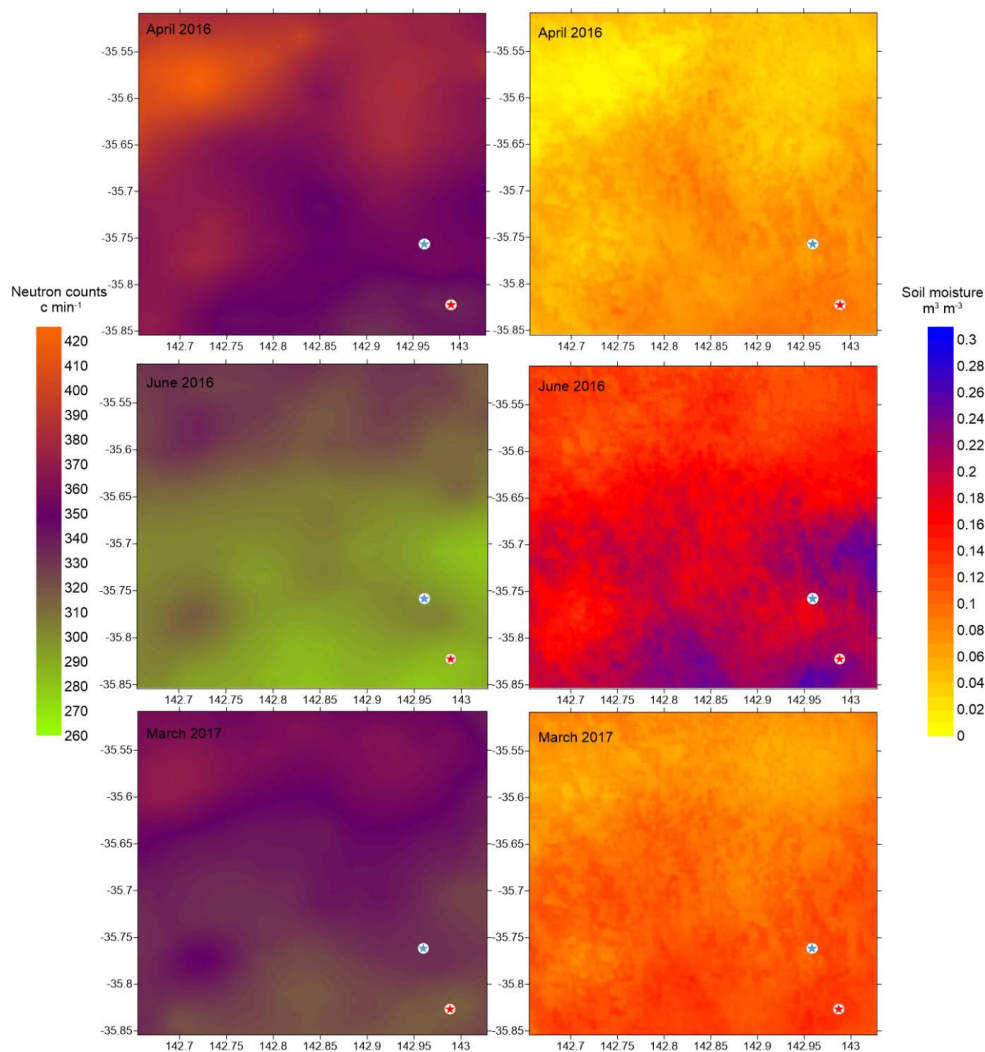
Figure 9. Location of target properties within the intensive scale survey area (red box) and property average soil moisture content for March 2017. Blue and red stars indicate the location of the Bishes and Bennetts cosmic-ray soil moisture sensors.



570

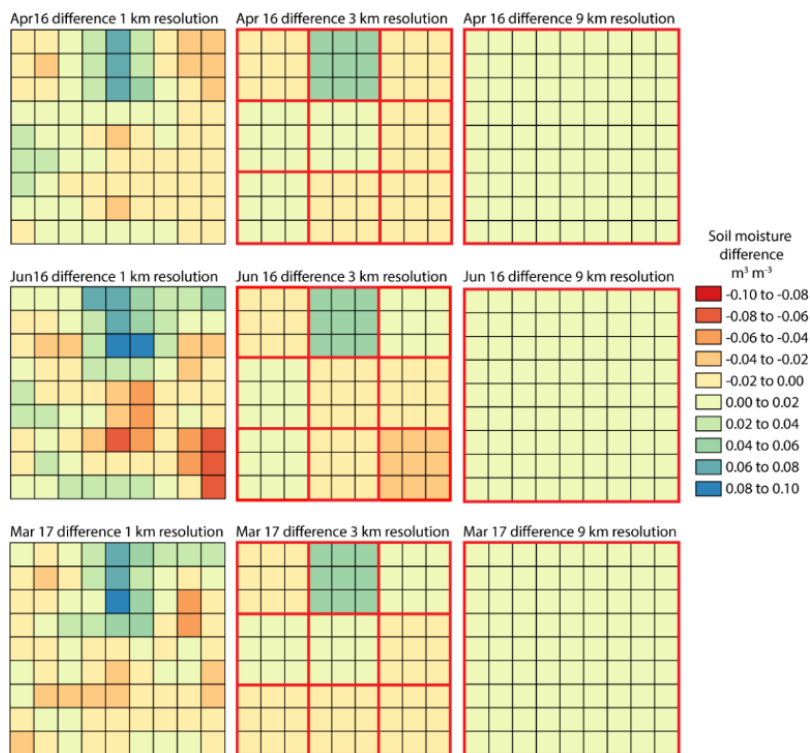
571 **Figure 10. Time series of average soil moisture for selected properties in the intensive scale survey area and**
572 **corresponding soil moisture time series from the Bennetts cosmic-ray soil moisture sensor. Scaling relationships are**
573 **provided in Table A1.**

574



575

576 **Figure 11. Interpolated counts (left column) and derived soil moisture (right column) for the three broad scale**
577 **surveys during April 2016, June 2016 and March 2017. Blue and red stars indicate the location of the Bishes and**
578 **Bennetts cosmic-ray soil moisture sensors.**



579

580

581

582

583

Figure 12. Difference in soil moisture estimates between the broad and intensive scale surveys for different resolutions on each of the three survey dates. Each cell represents a 1 km x 1 km region within the intensive survey zone.

584

585

586 **8 Appendix 1**587 **Table A1. Supplementary information from regression analysis relating CRNS observations to property average soil**
588 **moisture content in the intensive scale survey zone.**

Property	Soil Moisture ($\text{m}^3 \text{m}^{-3}$)			Regression modelling results		
	Apr-16	Jun-16	Mar-17	Slope	Intercept	R^2
<i>Bennetts CRNS</i>	0.124	0.277	0.157			
54 - Sandhill Central	0.065	0.152	0.080	0.575	-0.008	0.999
26 - Whirily	0.103	0.294	0.140	1.257	-0.055	1.000
34 - North West	0.070	0.199	0.095	0.848	-0.036	0.999
09 - Bennetts	0.097	0.264	0.139	1.076	-0.034	0.998
21 - Arnolds	0.079	0.216	0.147	0.809	-0.003	0.905
25 - School	0.082	0.222	0.136	0.858	-0.013	0.968
17 - Jil Jil East	0.077	0.181	0.097	0.685	-0.009	0.999
14 - Sandhill South	0.074	0.202	0.104	0.828	-0.027	1.000
24 - Box	0.079	0.223	0.118	0.922	-0.032	0.997
29 - Hancocks	0.086	0.210	0.139	0.749	0.006	0.947
13 - Billabong	0.092	0.254	0.128	1.052	-0.038	1.000
38 - 30 Acre	0.081	0.187	0.106	0.688	-0.003	1.000
18 - Barley	0.105	0.227	0.141	0.777	0.013	0.992
16 - Bishes East	0.027	0.132	0.057	0.674	-0.053	0.995
08 - Connelly's	0.093	0.223	0.123	0.845	-0.011	1.000
11 - South McKenzies	0.106	0.261	0.144	1.003	-0.016	0.999
32 - Far West	0.063	0.192	0.124	0.765	-0.016	0.919
36 - Bishes West	0.043	0.166	0.091	0.754	-0.040	0.962
40 - Watsons	0.092	0.222	0.125	0.839	-0.009	0.998
50 - Hogans	0.087	0.236	0.127	0.957	-0.028	0.996
51 - Hennessy's	0.089	0.254	0.159	1.000	-0.019	0.947
23 - O'Keefes	0.062	0.187	0.099	0.793	-0.031	0.992
22 - Alfies	0.071	0.197	0.108	0.801	-0.024	0.993
15 - Sandhill North	0.045	0.122	0.063	0.504	-0.017	0.999
35 - Jil Jil West	0.057	0.164	0.072	0.721	-0.036	0.995
30 - Hancocks Hill	0.054	0.188	0.128	0.770	-0.020	0.865
04 - Biggses	0.097	0.242	0.153	0.891	-0.002	0.964
41 - Front	0.095	0.193	0.127	0.620	0.023	0.985
03 - Perns	0.076	0.213	0.135	0.827	-0.013	0.945
45 - Dip	0.095	0.213	0.135	0.734	0.011	0.982
06 - Langs	0.091	0.290	0.125	1.316	-0.076	0.998
07 - Spittles	0.094	0.275	0.119	1.216	-0.063	0.993
05 - Rogers	0.084	0.224	0.121	0.896	-0.024	0.997
19 - Clovers East	0.095	0.274	0.170	1.093	-0.024	0.951
10 - Caldoes	0.081	0.205	0.129	0.758	-0.003	0.965
12 - North McKenzies	0.089	0.269	0.140	1.149	-0.048	0.995
27 - Jack Shehans	0.083	0.216	0.135	0.818	-0.007	0.966
42 - Warne	0.066	0.189	0.089	0.807	-0.035	0.999
44 - Windmill	0.077	0.220	0.147	0.848	-0.010	0.911
43 - Top	0.074	0.206	0.093	0.883	-0.040	0.995
37 - Barrell	0.095	0.206	0.129	0.701	0.013	0.991
48 - Vernies	0.082	0.200	0.103	0.781	-0.017	0.999
20 - Clovers South	0.086	0.221	0.139	0.830	-0.006	0.963
33 - Near West	0.067	0.206	0.106	0.889	-0.039	0.995
31 - Back Jack Shehans	0.070	0.215	0.125	0.896	-0.030	0.969
28 - Clovers West	0.093	0.260	0.166	1.004	-0.014	0.940
39 - Crossroads	0.077	0.214	0.126	0.855	-0.020	0.977
53 - Clovers North	0.079	0.229	0.151	0.893	-0.013	0.917

589

590